Published in final edited form as:
Nat Cell Biol. ; 14(4): 401–408. doi:10.1038/ncb2464.

Lrig1 controls intestinal stem cell homeostasis by negative regulation of ErbB signalling

Vivian W.Y. Wong[1,2,3,*], **Daniel E. Stange**[4,*], **Mahalia E. Page**[1,2,3,*], **Simon Buczacki**[5], **Agnieszka Wabik**[2], **Satoshi Itami**[6], **Marc van de Wetering**[4], **Richard Poulsom**[7,#], **Nicholas A. Wright**[7,8], **Matthew W.B. Trotter**[1,9,10], **Fiona M. Watt**[2,5,11], **Doug J. Winton**[5], **Hans Clevers**[4], and **Kim B. Jensen**[1,2,3]

[1]The Anne McLaren Laboratory for Regenerative Medicine, University of Cambridge, CB2 0SZ, UK [2]Wellcome Trust Centre for Stem Cell Research, University of Cambridge, Cambridge CB2 1QR, UK [3]Department of Oncology, University of Cambridge, CB2 0QQ, UK [4]Hubrecht Institute, KNAW and University Medical Center Utrecht, Uppsalalaan 8, 3584CT Utrecht, The Netherlands. [5]Cancer Research UK Cambridge Research Institute, Li Ka Shing Centre, Cambridge CB2 0RE, UK [6]Department of Regenerative Dermatology, Graduate School of Medicine, Osaka University, 2-2, Yamadaoka, Suita-shi, Osaka, 565-0871, Japan [7]Cancer Research UK - London Research Institute, London WC2A 3LY, UK [8]Barts and the London School of Medicine and Dentistry, London E1 2AD, UK [9]Department of Surgery, University of Cambridge, CB2 0QQ, UK [10]Celgene Institute Translational Research Europe, Seville E-41092, Spain [11]Department of Genetics, University of Cambridge, CB2 3EH, UK

Maintenance of adult tissues is carried out by stem cells and is sustained throughout life in a highly ordered manner[1,2]. Homeostasis within the stem cell compartment is governed by positive and negative feedback regulation of instructive extrinsic and intrinsic signals[3,4]. ErbB signalling is a prerequisite for maintenance of the intestinal epithelium following injury and tumour formation[5,6]. As ErbB family ligands and receptors are highly expressed within the stem cell niche[7], we hypothesise that strong endogenous regulators must control the pathway in the stem cell compartment. Here we show that Lrig1, a negative feedback regulator of the ErbB receptor family[8-10], is highly expressed by intestinal stem cells and controls the size of the intestinal stem cell niche by regulating the amplitude of growth factor signalling. Intestinal stem cell maintenance has so far been attributed to a combination of Wnt and Notch activation and Bmpr inhibition[11-13]. Our findings reveal ErbB activation as a strong inductive signal for stem cell proliferation. This has implications for our understanding of ErbB signalling in tissue development, maintenance and the progression of malignant disease.

The intestine constitutes an excellent system for studying stem cell function. Intestinal stem cells (ISC) reside at the bottom of crypts, where they are maintained in a multipotent and

Correspondence and requests for materials should be addressed to K.B.J. (kbj22@cam.ac.uk).
*These authors contributed equally to this work
#Present address: Centre for Digestive Disease, Blizard Institute, Barts and The London School of Medicine and Dentistry, Queen Mary University of London

Author contribution V.W.Y.W., D.E.S., H.C. and K.B.J. participated in the design of the study. K.B.J. wrote the manuscript. V.W.Y.W., D.E.S. M.E.P., S.B., A.W., M.v.d.W., M.W.B.T. and K.B.J performed experiments. S.I. and F.M.W. provided reagents. V.W.Y.W., D.E.S. M.E.P., F.M.W., M.W.B.T., D.J.W. and H.C. commented on manuscript. D.E.S., S.B., R.P., N.A.W., D.J.W., H.C. and K.B.J provided conceptual advice on study design and the interpretation of results.

Author information: The authors declare no competing financial interests.

Microarray data have been deposited at the EBI ArrayExpress under accession number: E-MTAB-378.

Europe PMC Funders Author Manuscripts

self-renewing state[14]. The ISC niche in the small intestine is composed of stem cells above and interspersed between Paneth cells and surrounded by mesenchymal cells[7,15]. This provides a unique microenvironment that enables constant contribution from stem cells to sustain the high cell turnover of the differentiated compartment[16,17]. Lgr5 expressing crypt based columnar cells at the bottom of crypts are together with cells located immediately above this region responsible for the life long steady state maintenance of the epithelium[14,15,18,19]. It is well established how ISCs are maintained and which inductive signals are required for tissue maintenance, however, very little is known with regard to the regulation of these pathways *in vivo*.

We recently demonstrated that Lrig1 controls stem cell proliferation in the epidermis[20]. *In situ* hybridisation now reveals that *Lrig1* is highly expressed in the stem cell niche of the small intestine and colon (Figure 1a; Supplementary Figure 1). Lgr5 expressing stem cells can be identified by their high levels of GFP in the *Lgr5*$^{-eGFP\text{-}ires\text{-}CreERT2}$ knock-in mouse[14]. GFP is subsequently diluted during successive cell divisions of stem cells (GFP^{high}) and their early daughter cells (GFP^{mid} and GFP^{low}). Expression analysis of these different populations demonstrates that *Lrig1* levels are highest within the ISCs (GFP^{high} vs. GFP^{mid}: 1.6x; GFP^{high} vs. GFP^{low}: 2.2x). Immunofluorescence staining and flow cytometric analysis confirm the overlap of Lrig1 and Lgr5 expression at the protein level and that Lrig1 is expressed in a gradient with highest levels in ISCs and that it is absent from Paneth cells (Figure 1b-c; Supplementary Figure 2a-c). Overall, approximately 1/3 of all cells within the intestinal crypt express Lrig1 (Figure 1d). This comprises the entire CD24$^{low/mid}$ stem cell and progenitor compartment and includes all of the Lgr5^{+ve} ISCs[21] (Figure 1e-g). The percentage of Lgr5-GFP^{+ve} cells within the Lrig1 expressing population can unfortunately not be determined due to the mosaic nature of the *Lgr5*$^{-eGFP\text{-}ires\text{-}CreERT2}$ knock-in mouse, where a large fraction of Lgr5 expressing ISCs are GFP negative (http://jaxmice.jax.org/strain/008875.html; Supplementary Figure 1). Characterisation of Lrig1^{+ve} cells isolated by flow cytometry demonstrates that markers, which define ISCs such as Lgr5, Ascl2 and Msi1, are all enriched in this population (Fig. 1h)[19,22]. We also observe differential expression of multiple transcripts for Lrig1 interaction partners, in particular *Egfr* (6.2x, Fig. 1h). Expression of Lrig1 is associated with reduced proliferation in other tissues[20]. Therefore, we test whether Lrig1 expressing cells are mainly quiescent or proliferative. Pulse-chase studies show that 15-20% of the Lrig1 expressing cells incorporate BrdU within 1 hour following one injection and 60% are labelled after a three-day pulse with 7 injections (Figure 1i). The BrdU label is subsequently lost or significantly reduced following a 1-week chase (Supplementary Figure 2d-e). We conclude that Lrig1 is highly expressed by all ISCs, that the majority of Lrig1 expressing cells are proliferating and that especially the expression of *Egfr* is enriched within the Lrig1^{+ve} population.

Work with Lrig1 knock out (KO) mice has until now been carried out on an outbred genetic mouse background[20,23]. To eliminate the contribution of genetic variability in the interpretation of the effects of Lrig1, we backcrossed Lrig1 KO mice to an Fvb/N background for more than 7 generations. On this background, no differences are observed between heterozygous and wildtype littermates. Yet, Lrig1 KO animals are smaller than their littermates from postnatal day 8 onwards and have to be sacrificed around postnatal day 10 due to the severity of the phenotype. Whilst the sizes of most organs are in relative proportion to the reduced body weight, the relative size of the intestine is grossly enlarged in Lrig1 KO mice (Figure 2a-d; circumference: 7.3±0.5mm for WT/Het (n=5) and 11.0±1.0mm for KO (n=4); p=0.01).

Histological examination of the intestine reveals that loss of Lrig1 causes a dramatic increase in crypt size along the entire length of the small intestine (Figure 2e-f; Supplementary Figure 3a). This is associated with an increased number of proliferating cells

as measured by expression of phospho-histone H3 (Figure 2g-h, pHistoneH3/crypt: 3.9±0.9 fold KO/ctrl, p=0.05). Phenotypically, crypts from KO mice and littermate controls are indistinguishable until postnatal day 6 (Supplementary Figure 3b). This coincides with stem cell specification in the neonatal intestinal epithelium[24]. Crypt hyperplasia can be observed from this time-point onwards in Lrig1 KO animals. Gene expression profiling reflects the phenotypic change associated with loss of Lrig1 as gene set enrichment analysis (GSEA) shows overrepresentation of crypt signature genes within the up-regulated genes ($p=1.5\times10^{-177}$)[25].

The enlarged crypt morphology can be explained by a specific increase in the transit-amplifying compartment, by a disproportionate increase in individual crypt cell lineages, or by increased numbers of ISCs with a proportionate increase in transit-amplifying and Paneth cells. The major intestinal cell lineages can be identified by their differential expression of CD24 and binding of *Ulex Europaeus* Agluttinin (UEA-I) by secretory cells (Supplementary Figure 4). Loss of Lrig1 causes a profound increase in the proportion of the $CD24^{low/mid}$/$UEA\text{-}I^{neg}$ stem cell and progenitor compartment (D) and $CD24^{high}$/$UEA\text{-}I^{pos}$ Paneth cells (B), whereas the population comprising mature enterocytes is proportionally decreased (C) (Figure 3a-b). Goblet (A) and enteroendocrine (E) cell populations show no significant change. In addition to their increased numbers, we observe increased expression of ISC markers within the $CD24^{low/mid}$/$UEA\text{-}I^{neg}$ population supporting an expansion of the stem cell compartment upon loss of Lrig1 (Figure 3c). To confirm this finding, we perform *in situ* hybridisation for *Olfm4*, a marker of ISCs[22], and *Cryptdin6*, a marker of Paneth cells[26]. Starting from postnatal day 6 we observe an increased number of *Olfm4* positive cells in Lrig1 KO samples and from postnatal day 10 an increased proportion of *Cryptdin6* positive Paneth cells (Figure 3d). The dynamic expansion of the stem cell compartment is supported by flow cytometric analysis of dissociated cells from the intestinal epithelium (Supplementary Figure 5a-e). The expression domain of the independent stem cell marker Msi1 is also expanded upon loss of Lrig1 (Supplementary Figure 5f-g). Taken together, this supports a direct effect of Lrig1 on ISCs, which subsequently affects the size of ISC compartment and the crypt.

Lrig1 interacts with the ErbB family, cRet and cMet *in vitro* and reduces signalling strength by negatively regulating both protein levels and the activity of the growth factor receptors[8-10,27,28]. Epithelial cells in the intestine express detectable levels of Egfr, ErbB2, ErbB3 and cMet (Figure 1h and 4a). ErbB signalling is mediated via ligand stimulation of Egfr and ErbB3, which upon homo- and heterodimerisation with each other or with the orphan receptor ErbB2 activates downstream signalling cascades[29]. cMet on the other hand is activated upon HGF stimulation. Loss of Lrig1 causes a pronounced increase in the protein levels of all of these interaction partners irrespective of transcript levels (Figure 4a-b). This is associated with a concomitant increase in the activity of the ErbB family, but with no detectable effect on the activation of cMet (Figure 4a and data not shown). The increased ErbB activation is reflected by strong up-regulation of MAPK signalling and increased levels and activity of the mitogen-induced transcription factor cMyc (Figure 4c-f; GSEA of the Myc dependent gene network[30]: $p=3.0\times10^{-18}$). In order to address whether the increased levels of ErbB signalling reflects merely the expansion of the crypt or if loss of Lrig1 alters signalling dynamics we utilise two independent approaches. Firstly, phosphorylation of Egfr (pEgfr) is a direct measure for receptor activation *in vivo*. At postnatal day 10 phosphorylation can be observed on $UEA\text{-}1^{pos}$ secretory cells and progenitor cells (Supplementary Figure 6). In control animals, pEgfr levels are low at the crypt bottom and peak around cell position 8 (Figure 4g,i). Of note, this is the reverse expression pattern of Lrig1. In the Lrig1 KO, Egfr activation is uniform within the crypt (Figure 4h,i). Secondly, expression analysis of isolated cell populations signifies the increased activation of Myc

within ISCs and progenitors upon loss of Lrig1 (Figure 4j). We conclude that loss of Lrig1 affects ErbB signalling within the ISC compartment.

Next, we functionally test in a defined 3D intestinal culture system whether ErbB inhibition is the main function of Lrig1. ISC self-renewal and proliferation require stimulation of the Egfr and the Wnt pathways, and inhibition of the Bmpr pathway[31]. In wild type samples, stimulation of ErbB signalling with exogenous ligands is a prerequisite for the maturation from spheres into budding organoids. Interestingly, Lrig1 KO spheres mature into budding organoids in the absence of exogenous ErbB ligands (Figure 4k-l). Nevertheless, ErbB signalling, like stimulation of the Wnt pathway and inhibition of BMPR signalling, is an obligate requirement for growth of both WT and KO organoids, as inhibition of ErbB signalling with a number of ErbB inhibitors rapidly affects cell survival (data not shown). Importantly, loss of Lrig1 does not cause increased expression of ErbB ligands (Figure 4m). We conclude that upon loss of Lrig1, endogenous ErbB ligands are sufficient to support organoid growth due to reduced ErbB inhibition in ISC. Moreover, as the phenotype observed *in vivo* can be recapitulated *in vitro* in a purely epithelial culture, the function of Lrig1 is likely to be crypt autonomous.

To address *in vivo* whether activation of the ErbB family is responsible for the observed phenotype, neonatal mice were treated daily with the ErbB inhibitor Gefitinib. Following administration of inhibitor *in vivo*, crypt proliferation as well as ISC and Paneth cell numbers is restored to normal levels in the Lrig1 KO animals (Figure 5a-l). Moreover, treatment with Gefitinib reduces pEgfr levels (Figure m-p). Gefitinib-treated KO animals are still significantly smaller than control animals, and we hypothesise that Lrig1 has important non-reversible functions in other tissues such as the stomach, where Lrig1 is expressed by a small sub-population of cells within the pyloric glands (M.P. and K.B.J. Unpublished observations). The proposed mechanism of Lrig1 as an inhibitor of ErbB function *in vivo* is further substantiated by genetic rescue of the phenotype by crossing Lrig1 KO animals to hypomorphic $Egfr^{wa\text{-}2}$ mice (Figure 5q-t). The $Egfr^{wa\text{-}2}$ mouse strain harbours a missense mutation in the kinase domain of Egfr, which compromises the activity of the receptor upon ligand stimulation[32]. Homozygosity for $Egfr^{wa\text{-}2}$, when crossed with Lrig1 KO mice, is associated with perinatal lethality irrespective of Lrig1 status. Analysis of the $Egfr^{wa\text{-}2}$ heterozygous animals at postnatal day 10 demonstrates that the phenotypical changes associated with loss of Lrig1 are rescued in approximately 40% of the mice (n=15 out of 37, p=0.0095). Thus, the phenotypical changes observed upon loss of Lrig1 can be rescued by both pharmacological and genetic modulation of endogenous ErbB activity, hereby demonstrating ErbB activity as the main target of Lrig1 *in vivo*.

Our data support a model whereby Lrig1 regulates proliferation within the ISC niche by inhibiting ErbB signalling. Expression of Lrig1 enables stem cells and progenitors to fine-tune their cellular response upon ligand stimulation and ensures that tissue homeostasis is maintained (Figure 5u). Proliferation and maintenance of the ISC compartment have until now been attributed to Wnt and Notch activation in combination with BMPR inhibition[11-13]. We show that ErbB signalling is a strong mitotic signal for ISCs, and when uninhibited leads to a rapid expansion of the stem cell compartment. The prominent role of ErbB signalling in the ISC compartment is supported by recent evidence from Drosophila, where signalling via Egfr, the only ErbB receptor in Drosophila, is required for intestinal maintenance[33,34]. Moreover, the natural response to injury and tumour initiation in the mouse intestine, which includes stem cell activation, is severely compromised upon loss of Egfr and ErbB3[5,6]. Analogous to our observations, eliminating one functional copy of the Egfr significantly alters the injury response to sub-lethal doses of radiation[35]. In the case of injury models it remains to be shown whether Egfr and ErbB3 function is required for expansion of the stem cell compartment or as a general mitotic stimuli.

Due to the reported anti-proliferative effect of Lrig1 in human and murine epidermis[9,20], we have assessed the proliferation status of Lrig1 expressing cells. As predicted from the overlap in Lrig1 and Lgr5 expression, we observe that the majority of Lrig1 expressing cells like $Lgr5^{+ve}$ cells are highly proliferative. We cannot rule out that mitotic heterogeneity exists within the $Lrig1^{+ve}$ population; however, it is evident that Lrig1 does not define a population of quiescent cells in the intestine. The prominent effect on the stem cell compartment upon loss of Lrig1 does however highlight that ISCs are exposed to multiple signals that promote proliferation and that distinct inhibitory factors like Lrig1 are required to control stem cells.

We unambiguously demonstrate that Lrig1 is a key regulator of tissue homeostasis in the intestinal epithelium. As multiple tissue-specific stem cells rely on Lrig1 to regulate their behaviour, we propose that Lrig1 provides a general mechanism to control tissue homeostasis. Based on the study described here, and the non-overlapping expression pattern of Lrig1 and Lgr5 in stem cells of the epidermis[20,36], we anticipate that distinct cellular microenvironments, which can either converge as in the intestine or diverge as in the epidermis, specify stem cell behaviour *in vivo*.

Methods section

Mice

FVB/N mice were obtained from Charles River. Lrig1 KO mice[23], $Egfr^{wa\text{-}2}$ and $Lgr5^{-EGFP\text{-}IRES\text{-}CreERT2}$ knock in mice[14] have been described. $Egfr^{Wa\text{-}2}$ mice crossed to Fvb/N for 1 generation were bred with Lrig1 KO. The offspring was subsequently intercrossed in order to obtain Lrig1 KO mice on the hypermorphic $Egfr^{wa\text{-}2}$ background. For DNA labelling experiments mice received single or repeated intraperitoneal injections of 100μL 10mg/mL BrdU (10mg/mL) every 12-hour. For experiments with Gefitinib (Cambridge Bioscience, Cambridge, UK), neonatal mice received daily intraperitoneal injections of 20μg/g bodyweight of Gefitinib. All *in vivo* experiments were performed under the terms of a UK Home Office license.

Tissue preparation

Intestinal samples were fixed and embedded in paraffin using standard protocols. Analysis of Lgr5-GFP/Lrig1 and UEA-1/pEgfr was carried out as recently described[22].

Antibodies

The following antibodies were used rabbit anti-β-catenin (Santa Cruz, sc-7199, 1:250), rabbit anti-Phospho-histone H3 (ser10) (Cell Signaling #9701, 1:400), rabbit anti-phospho-MEK1/2 (Ser221) (Cell signalling, #2338, 1:500), mouse anti-BrdU (Cell signaling, Bu20a, 1:250), goat anti-Lrig1(R and D Systems, AF3688, 1:100), rabbit anti-Myc (Millipore, 06-340, 1:100), mouse anti-Ki67 (Monosan, Clone MM1, 1:1000), PE-conjugated anti-Lrig1 (R and D systems, FAB3688P, $10\mu L/10^6$ cells), Pacific blue and Alexa647 conjugated Rat anti-CD24 (Biolegend, M1/69, $5\mu L/10^6$ cells), rat anti-Msi1 (MBL, D270-6, 1:10000), rabbit anti-phospho Egfr (Y1068) (Abcam, EP7774Y, 1:250), rabbit anti-Egfr (Cell Signaling, #4267 clone D38B1, 1:250), rabbit anti-phospho ErbB2 (Y1248) (Abcam, ab47755), mouse anti-ErbB2 (Millipore, 05-1130, Clone N3D10, 1:500), rabbit anti-phospho ErbB3 (Y1289) (Cell Signaling, #4791, Clone 21D3, 1:250), mouse anti-ErbB3 (Millipore, 05-390, Clone 2F12, 1:500), rabbit anti-cMet (Santa Cruz, sc-162, 1:500), mouse anti-β-actin, (Sigma A5316, clone AC-74, 1:5000) and Atto-488 conjugated UEA-1 (Sigma, $10\mu L/10^6$ cells for flow cytometry, 1:1000 for near-native sections) according to manufacturer's instructions. For confocal microscopy samples were imaged using a LSM700 confocal microscope or Leica SP5 TCS. Z-stacks were acquired at optimal stack

distance and at 1024×1024 dpi resolution. Maximum intensity projections of Z-stacks were generated in Image J.

RNA extraction and qPCR

One cm pieces of the jejunum from postnatal day 10 Lrig1 KO and control littermates were rinsed with ice cold PBS and snap frozen on dry ice. RNA was isolated from homogenised intestine or flow-sorted cells and either used directly for microarray experiments or for qPCR as described[20].

Gene specific expression assays (Applied Biosystems) or Sybr green analysis (Invitrogen) with optimised primer-pairs were used for qPCR on an Applied Biosystems 7500HT RealTime PCR System (Applied Biosystems, Foster,USA). Samples were normalised using the ΔCt method. For clustering analysis average expression levels from at least three independent biological replicates were converted to z-scores (z=(value-average value)/stdev) and plotted using heatmap.2′ function from the Bioconductor 'gplots' library.

Microarray Analysis

RNA was quality controlled for concentration, purity and integrity using spectroStar omega (BMG labtech) and Bioanalyser (Agilent). The amplification was performed using the TotalPrep 96-RNA Amplification kit (Ambion). Total RNA (~300ng) was reverse transcribed into cDNA and amplified by *in vitro* transcription to generate biotin-labelled cRNA. cRNA (1500 ng) was hybridised to whole genome bead arrays (MouseWG-6 v2.0 Expression BeadChip) according to the direct hybridisation assay from Illumina and scanned using an Illumina BeadArray scanner. Bead level data from all hybridizations was background corrected, using default parameters of the RMA algorithm[37], and summarised using the *beadarray* package for the Bioconductor suite (http://www.bioconductor.org) for the *R* statistical programming environment (http://www.r-project.org). Processed sample expression profiles were quantile normalised using the *limma* package for Bioconductor prior to analysis of differential regulation between sample groups with the moderated t-statistic of the same package[38]. In order to reduce errors associated with multiple hypothesis testing, the significance p-values obtained were converted to corrected q-values using the false discovery rate (FDR) method[39], as implemented in the *qvalue* package for Bioconductor. Differential regulation between two sample groups was deemed significant at a threshold of $q < 0.01$ (FDR 1%, Supplementary Table 1).

In order to generate a reference gene universe for gene set enrichment analysis we defined the intestinal transcriptome as genes detected in three replicates from KO and control samples (13,298 unique genes, 2,575 up-regulated genes, 2,553 down-regulated genes; Supplementary Table 2). For GSEA using Fisher's exact test we obtained a crypt gene signature[25] (1,692 genes in reference list, 802 genes up-regulated; Supplementary Table 3) and a Myc dependent gene network[30] (374 genes in reference list, 144 genes up-regulated; Supplementary Table 4).

Western blot analysis and *in situ* hybridisation

For protein isolation, intestinal epithelium was extracted as for organoid cultures and lysed in RIPA buffer.

DIG *in situ* hybridisation was carried out essentially as described before using IMAGE clones[40].

Europe PMC Funders Author Manuscripts

Flow cytometry

Intestinal epithelial cells were isolated as described[22]. To generate a single cell suspension, cells were incubated with trypsin[22] or with 0.25mg/mL Thermolysin for 1 minute at 37°C in PBS supplemented with 1%BSA for trypsin sensitive antigens such as Lrig1. Cell sorting was carried out using a FACSAria (BD Biosciences) for isolation of cells based on CD24 and UEA-1, and a MoFlo (Dako Cytomation) for isolation of Lrig1 and Lgr5-eGFP expressing cells. Flow cytometric analysis was carried out on a CyAn ADP analyzer (Dako Cytomation), and data was processed in FlowJo.

The BrdU labelling analysis was performed with the APC-BrdU flow cytometry kit (BD biosciences).

Organoid cultures

Primary crypts were cultured according to Sato et al.[31] using reduced concentrations of murine recombinant R-spondin1 (500ng/mL – R&D Systems) and varying concentrations of EGF (Peprotech). Organoid structures were imaged at day 6. Cell proliferation was measured by BrdU incorporation by incubation with 20μM BrdU (Roche) for 1 hour at 37°C before fixation.

Image analysis

Confocal images of intestinal samples stained for pEgfr were analysed in ImageJ to determine the levels of membrane-localised pEgfr. Intra-crypt intensities were normalised to the average intensity of position 6-10. This corresponds to the peak in control samples.

Organoids in matrigel were observed under phase contrast using an Axiovert 200M microscope (Zeiss) equipped with an AxioCam MRc (Zeiss). Images were interactively analyzed using ImageJ to determine perimeter and area of individual organoids and calculate the branching coefficient ($1\text{-}4\pi(\text{Area}/\text{perimeter}^2)$) of the formed structures. Images were acquired from a minimum of 8 organoids per condition derived from independent KO and control samples,

Statistical analysis

Statistical significance of quantitative data was determined by applying a two-tailed Student's t-test to raw values or to the average values obtained from analysis of independent organoid experiments. A two-tailed Fisher's exact test was used to analyse the significance of the genetic rescue of the Lrig1 KO phenotype, and to determine the significant overlap between different gene lists.

Supplementary Material

Refer to Web version on PubMed Central for supplementary material.

Acknowledgments

We thank Erwin Wagner, Michaela Frye, Stuart Yuspa, Bill Otto, Rachael Walker, Rosemary Jeffery, Harry Begthel, Margaret McLeish, the WTCSCR Biofacility and Cambridge Genomics Services for reagents, technical assistance and advice, and Robert Fordham and Robert Williams for critical comments on the manuscript. We gratefully acknowledge support from the MRC and Wellcome Trust.

References

1. Blanpain C, Horsley V, Fuchs E. Epithelial stem cells: turning over new leaves. Cell. 2007; 128:445–458. [PubMed: 17289566]

2. Morrison SJ, Spradling AC. Stem cells and niches: mechanisms that promote stem cell maintenance throughout life. Cell. 2008; 132:598–611. [PubMed: 18295578]
3. Li L, Clevers H. Coexistence of quiescent and active adult stem cells in mammals. Science. 2010; 327:542–545. [PubMed: 20110496]
4. Voog J, Jones DL. Stem cells and the niche: a dynamic duo. Cell Stem Cell. 2010; 6:103–115. [PubMed: 20144784]
5. Lee D, et al. Tumor-specific apoptosis caused by deletion of the ERBB3 pseudo-kinase in mouse intestinal epithelium. J Clin Invest. 2009; 119:2702–2713. [PubMed: 19690388]
6. Roberts RB, et al. Importance of epidermal growth factor receptor signaling in establishment of adenomas and maintenance of carcinomas during intestinal tumorigenesis. Proc Natl Acad Sci U S A. 2002; 99:1521–1526. [PubMed: 11818567]
7. Sato T, et al. Paneth cells constitute the niche for Lgr5 stem cells in intestinal crypts. Nature. 2011; 469:415–418. [PubMed: 21113151]
8. Gur G, et al. LRIG1 restricts growth factor signaling by enhancing receptor ubiquitylation and degradation. Embo J. 2004; 23:3270–3281. [PubMed: 15282549]
9. Jensen KB, Watt FM. Single-cell expression profiling of human epidermal stem and transit-amplifying cells: Lrig1 is a regulator of stem cell quiescence. Proc Natl Acad Sci U S A. 2006; 103:11958–11963. [PubMed: 16877544]
10. Laederich MB, et al. The leucine-rich repeat protein LRIG1 is a negative regulator of ErbB family receptor tyrosine kinases. J Biol Chem. 2004; 279:47050–47056. [PubMed: 15345710]
11. Haramis AP, et al. De novo crypt formation and juvenile polyposis on BMP inhibition in mouse intestine. Science. 2004; 303:1684–1686. [PubMed: 15017003]
12. Korinek V, et al. Depletion of epithelial stem-cell compartments in the small intestine of mice lacking Tcf-4. Nat Genet. 1998; 19:379–383. [PubMed: 9697701]
13. van Es JH, et al. Notch/gamma-secretase inhibition turns proliferative cells in intestinal crypts and adenomas into goblet cells. Nature. 2005; 435:959–963. [PubMed: 15959515]
14. Barker N, et al. Identification of stem cells in small intestine and colon by marker gene Lgr5. Nature. 2007; 449:1003–1007. [PubMed: 17934449]
15. Tian H, et al. A reserve stem cell population in small intestine renders Lgr5-positive cells dispensable. Nature. 2011; 478:255–259. [PubMed: 21927002]
16. Lopez-Garcia C, Klein AM, Simons BD, Winton DJ. Intestinal Stem Cell Replacement Follows a Pattern of Neutral Drift. Science. 2010; 330:822–825. [PubMed: 20929733]
17. Snippert HJ, et al. Intestinal crypt homeostasis results from neutral competition between symmetrically dividing Lgr5 stem cells. Cell. 2010; 143:134–144. [PubMed: 20887898]
18. Takeda N, et al. Interconversion between intestinal stem cell populations in distinct niches. Science. 2011; 334:1420–4. [PubMed: 22075725]
19. Sangiorgi E, Capecchi MR. Bmi1 is expressed in vivo in intestinal stem cells. Nat Genet. 2008; 40:915–920. [PubMed: 18536716]
20. Jensen KB, et al. Lrig1 expression defines a distinct multipotent stem cell population in mammalian epidermis. Cell Stem Cell. 2009; 4:427–439. [PubMed: 19427292]
21. von Furstenberg RJ, et al. Sorting mouse jejunal epithelial cells with CD24 yields a population with characteristics of intestinal stem cells. Am J Physiol Gastrointest Liver Physiol. 2011; 300:G409–417. [PubMed: 21183658]
22. van der Flier LG, et al. Transcription factor achaete scute-like 2 controls intestinal stem cell fate. Cell. 2009; 136:903–912. [PubMed: 19269367]
23. Suzuki Y, et al. Targeted disruption of LIG-1 gene results in psoriasiform epidermal hyperplasia. FEBS Lett. 2002; 521:67–71. [PubMed: 12067728]
24. Schmidt GH, Winton DJ, Ponder BA. Development of the pattern of cell renewal in the crypt-villus unit of chimaeric mouse small intestine. Development. 1988; 103:785–790. [PubMed: 3248525]
25. Chong JL, et al. E2f1-3 switch from activators in progenitor cells to repressors in differentiating cells. Nature. 2009; 462:930–934. [PubMed: 20016602]

26. van Es JH, et al. Wnt signalling induces maturation of Paneth cells in intestinal crypts. Nat Cell Biol. 2005; 7:381–386. [PubMed: 15778706]
27. Shattuck DL, et al. LRIG1 is a novel negative regulator of the Met receptor and opposes Met and Her2 synergy. Mol Cell Biol. 2007; 27:1934–1946. [PubMed: 17178829]
28. Ledda F, Bieraugel O, Fard SS, Vilar M, Paratcha G. Lrig1 is an endogenous inhibitor of Ret receptor tyrosine kinase activation, downstream signaling, and biological responses to GDNF. J Neurosci. 2008; 28:39–49. [PubMed: 18171921]
29. Citri A, Yarden Y. EGF-ERBB signalling: towards the systems level. Nat Rev Mol Cell Biol. 2006; 7:505–516. [PubMed: 16829981]
30. Kim J, et al. A Myc network accounts for similarities between embryonic stem and cancer cell transcription programs. Cell. 2010; 143:313–324. [PubMed: 20946988]
31. Sato T, et al. Single Lgr5 stem cells build crypt-villus structures in vitro without a mesenchymal niche. Nature. 2009; 459:262–265. [PubMed: 19329995]
32. Luetteke NC, et al. The mouse waved-2 phenotype results from a point mutation in the EGF receptor tyrosine kinase. Genes Dev. 1994; 8:399–413. [PubMed: 8125255]
33. Biteau B, Jasper H. EGF signaling regulates the proliferation of intestinal stem cells in Drosophila. Development. 2011; 138:1045–1055. [PubMed: 21307097]
34. Jiang H, Grenley MO, Bravo MJ, Blumhagen RZ, Edgar BA. EGFR/Ras/MAPK signaling mediates adult midgut epithelial homeostasis and regeneration in Drosophila. Cell Stem Cell. 2011; 8:84–95. [PubMed: 21167805]
35. Iyer R, Thames HD, Tealer JR, Mason KA, Evans SC. Effect of reduced EGFR function on the radiosensitivity and proliferative capacity of mouse jejunal crypt clonogens. Radiother Oncol. 2004; 72:283–289. [PubMed: 15450726]
36. Jaks V, et al. Lgr5 marks cycling, yet long-lived, hair follicle stem cells. Nat Genet. 2008; 40:1291–1299. [PubMed: 18849992]
37. Irizarry RA, et al. Summaries of Affymetrix GeneChip probe level data. Nucleic Acids Res. 2003; 31:e15. [PubMed: 12582260]
38. Smyth GK. Linear models and empirical bayes methods for assessing differential expression in microarray experiments. Stat Appl Genet Mol Biol. 2004; 3 Article3.
39. Storey JD, Tibshirani R. Statistical significance for genomewide studies. Proc Natl Acad Sci U S A. 2003; 100:9440–9445. [PubMed: 12883005]
40. Gregorieff A, et al. Expression pattern of Wnt signaling components in the adult intestine. Gastroenterology. 2005; 129:626–638. [PubMed: 16083717]

Europe PMC Funders Author Manuscripts

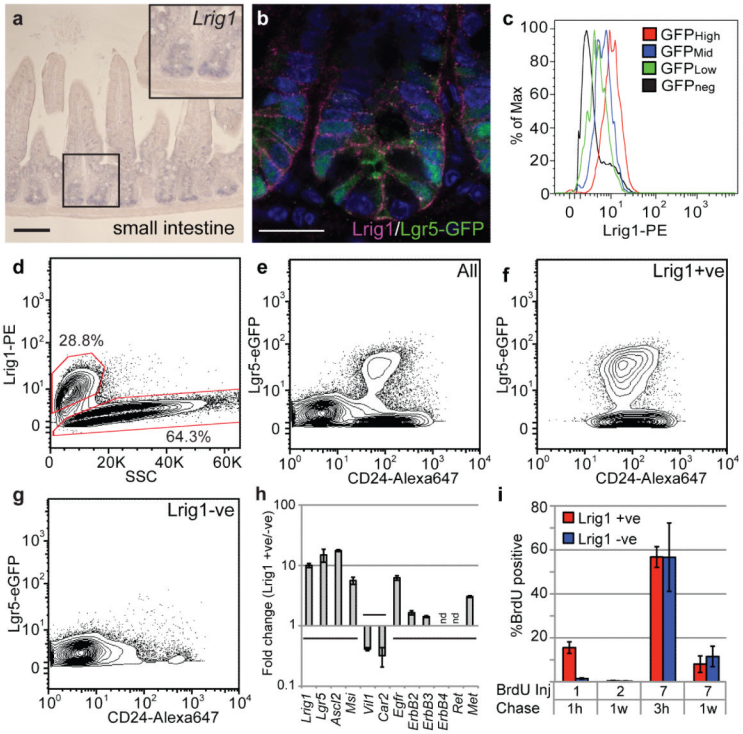

Figure 1. Characterisation of Lrig1 expression in the intestine

a) *In situ* hybridisation for *Lrig1* in adult mouse small intestine. Insert shows highest expression in the stem cell niche. **b)** Indirect immunofluorescence analysis for Lrig1 (magenta) and Lgr5-eGFP (green) in adult intestine of Lgr5$^{-eGFP\text{-}IRES\text{-}CreERT2}$ mice. Of note Paneth cells do not express Lrig1, the visible membrane staining of ISCs originates from only one cell membrane, whereas in the progenitor compartment the staining is a composite of two neighbouring cell membranes. **c)** Analysis of Lrig1 expression in Lgr5-GFP$^{high/mid/low}$ and GFP^{neg} populations from Lgr5$^{-eGFP\text{-}IRES\text{-}CreERT2}$ mice. **d)** Lrig1 is expressed by approximately 30% of all crypt cells as determined by flow cytometry. **e)** Lgr5-GFP expressing cells express low to medium levels of CD24. **f)** All Lgr5-GFP expressing cells are Lrig1 positive, and both Lgr5-GFP and Lrig1 expressing cells fall in the CD24$^{low/mid}$ range. **g)** Lrig1 negative cells are either CD24^{high} or negative and Lgr5-GFP negative. **h)** Relative expression analysis by qPCR for ISC markers, differentiation markers and Lrig1 interaction partners in Lrig1 expressing vs. Lrig1 non-expressing cells. Error bar represents the s.e.m. of four independent samples. nd – not detected. **i)** Summary of flow cytometric analysis for BrdU in Lrig1 expressing and non-expressing cells following one or several injections of BrdU (BrdU Inj) and analysis following a 1h, 3h, and 1w chase. Error bars represent s.d. from four independent samples. Scale bars: 100μm (a), 25μm (b).

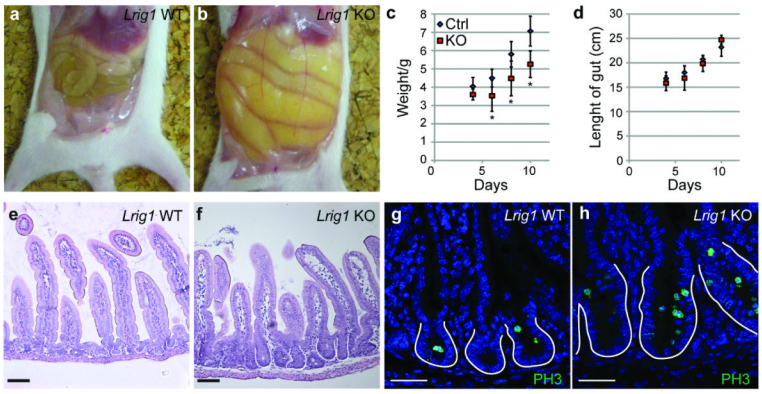

Figure 2. Loss of Lrig1 causes crypt expansion

a-b) Grossly enlarged abdomen in postnatal day 10 Lrig1 KO animals. **c-d)** Lrig1 KO animals are smaller than control littermates but the length of the gut is not affected. Length of the gut and weight of neonates collected from P4 to P10. (P4:WT/Het n=7, KO n=3; P6:WT/Het n=15; KO:n=7; P8:WT/Het n=9, KO n=5; P10:WT/Het n=16, KO n=7). Error bars represent s.d. and asterisks significant changes (P6: p=0.0028; P8: p=0.011; P10: $p=5.5\times10^{-5}$). **e-f)** Loss of Lrig1 causes crypt expansion. H&E staining of proximal jejunum from Lrig1 WT and KO littermates. White lines demarcate crypt structures. **g-h)** The crypts from Lrig1 KO animals contain more proliferating cells. Phosphorylated histone H3(Ser10) (green) in intestinal samples from Lrig1 WT and KO littermates counterstained with dapi (blue). Scale bars 100μm (e-f), 50μm (f-g).

Europe PMC Funders Author Manuscripts

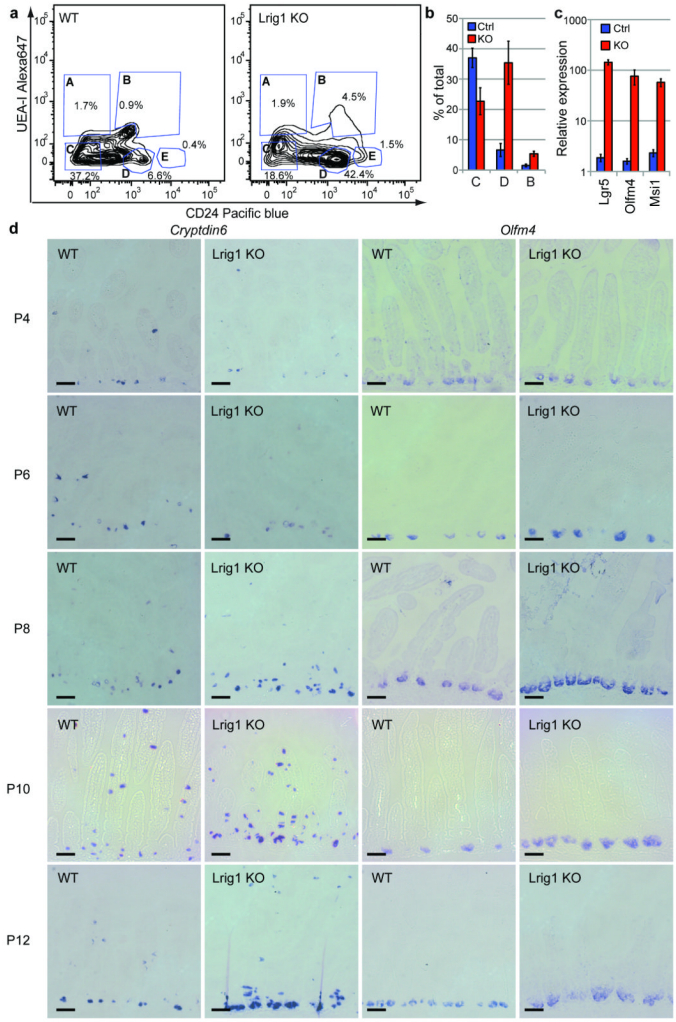

Figure 3. Loss of Lrig1 causes crypt and stem cell expansion

a) Dissection of epithelial lineages by flow cytometry based on the relative levels of CD24 and binding of UEA-I. The five identifiable population are enriched in A: Goblet cells (CD24^{neg}/UEA-I^{pos}), B: Paneth cells (CD24^{pos}/UEA-I^{pos}); C: transit-amplifying cells/ enterocytes (CD24^{neg}/UEA-I^{neg}); D: stem cells and progenitors (CD24$^{low/mid}$/UEA-I^{neg}); E: enteroendocrine cells (CD24^{high}/UEA-I^{neg}). **b)** Loss of Lrig1 leads to a disproportionate increase in CD24^{pos}/UEA-I^{pos} Paneth cells and CD24$^{low/mid}$/UEA-I^{neg} stem cells and progenitors. Error bars represent s.d. from 4 control and 3 Lrig1 KO samples (CD24^{neg}/ UEA-I^{neg} transit-amplifying cells/enterocytes: p=4.1×10^{-3}; CD24$^{low/mid}$/UEA-I^{neg} stem cells and progenitors: p=5.3×10^{-4}; CD24^{pos}/UEA-I^{pos} Paneth cells: p=4.7×10^{-4}). **c)** Enrichment of stem cell markers in the CD24$^{low/mid}$/UEA-I^{neg} stem cells and progenitors upon loss of Lrig1. Error bars represent the s.e.m. from 3 Lrig1 KO and 4 control samples (*Lgr5*: p=2×10^{-4}; *Olfm4*: p=0.02; *Msi1*: p=0.001). **d)** Loss of Lrig1 causes a progressive expansion of the stem cell niche from postnatal day 6 as detected by *in situ* hybridisation for *Olfm4* and *Cryptdin6*, respectively. Scale bars 50μm.

Europe PMC Funders Author Manuscripts

Europe PMC Funders Author Manuscripts

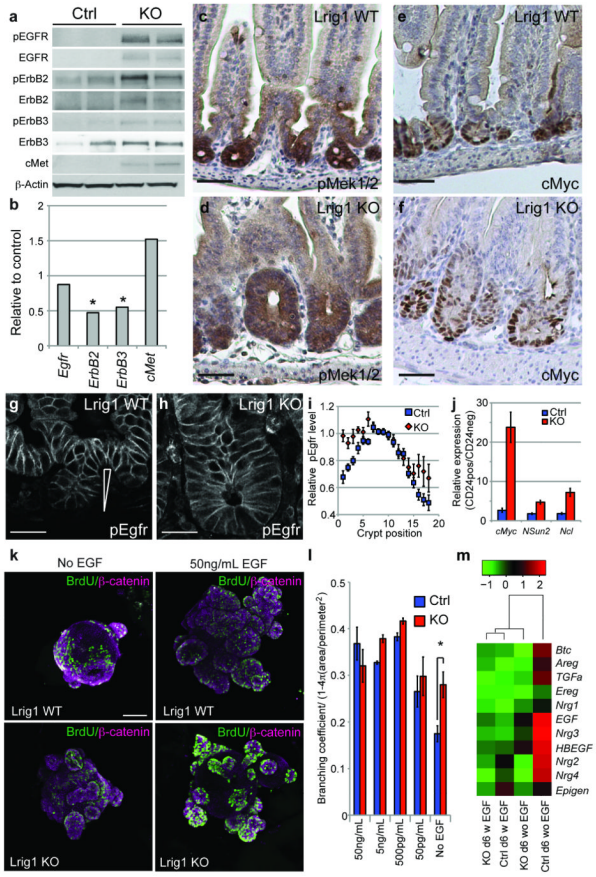

Figure 4. Lrig1 controls endogenous signalling via the ErbB pathway

a) Loss of Lrig1 causes increased protein levels and activation of the ErbB pathway. pEgfr, Egfr, pErbB2, ErbB2, pErbB3, ErbB3, cMet were detected by Western blotting in samples enriched for intestinal epithelium. β-actin is used a loading control. **b)** Relative expression analysis of the receptors by qPCR at P10 shows minor differences. Expression levels are shown relative to control samples (KO/Ctrl). Asterisks indicate significant changes (*ErbB2*: p=0.004; *ErbB3*: p=0.04; KO n=4, Ctrl n=3). **c-f)** Increased activation of MAPK signalling and cMyc signalling upon loss of Lrig1. Immunohistochemical analysis for p-MEK1-2 (c-d) and cMyc (e-f). **g-i)** Altered Egfr activation dynamics upon loss of Lrig1 KO. **i)** Average normalised membrane intensity of pEgfr in intestinal samples from KO (n=6) and control animals (n=10) for 6-18 individual crypts per sample. Error bars represent the s.e.m. (positions 1-4: $p<0.05$). **j)** Increased Myc activity in progenitors lacking Lrig1. Relative expression of *Myc* and Myc target genes in $CD24^{low/mid}$/UEA-I^{neg} stem cells and progenitors versus $CD24^{neg}$/UEA-I^{neg} transit-amplifying cells/enterocytes from control (n=4) and Lrig1 KO (n=3) tissues. Error bar represent the s.e.m. (*Myc*: p=0.001; *NSun2*: p=0.001; *Ncl*: p=0.002). **k)** Lrig1 KO organoids mature in the absence of exogenous ErbB ligands. Maximum intensity projection of confocal images of WT and KO organoids shows incorporation of BrdU (green) and β-catenin as counterstain (magenta). **l)** EGF signalling is required for organoid maturation. The branching coefficient was determined for varying concentrations of EGF for independently derived samples (n=3 for all except for 50ng/mL and no EGF: n between 6 and 9). Error bars represent the s.e.m. and asterisk significant change (p=0.009). **m)** Loss of Lrig1 does not affect ErbB ligand expression. The relative levels of ErbB ligands were determined by qPCR on material from organoids grown for 2 and 6 days with or without EGF. Red and green colours reflect increased and decreased

deviation from the mean, respectively. The dendogram indicates that ctrl samples grown for 6 days in normal conditions cluster with Lrig1 KO samples grown with and without EGF. Scale bars 50μm (c-h) and 100μm (a-d).

Europe PMC Funders Author Manuscripts

Europe PMC Funders Author Manuscripts

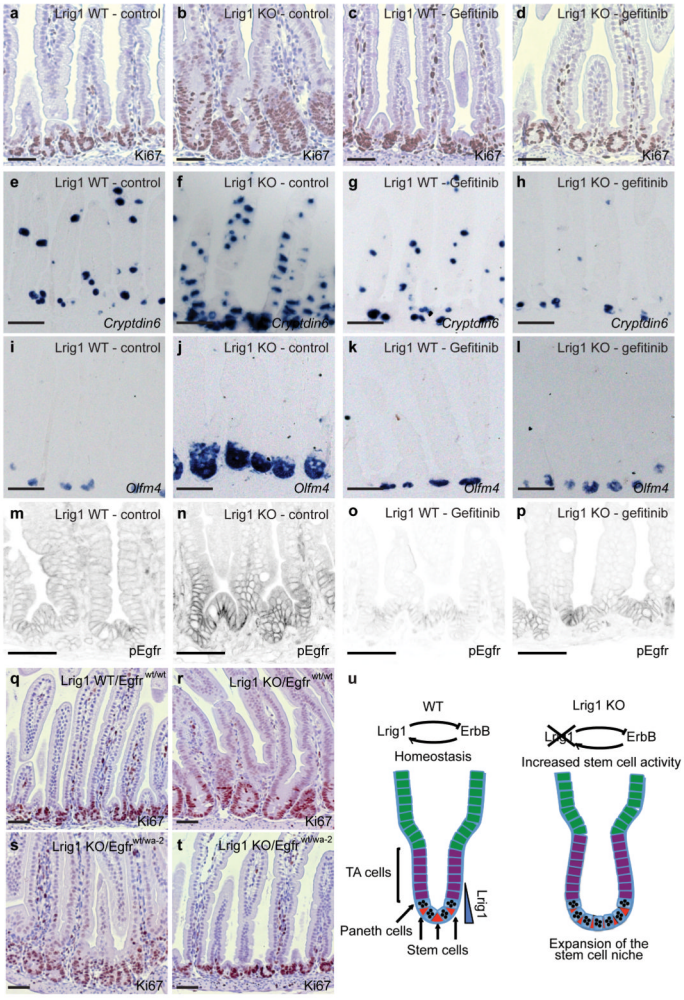

Figure 5. Lrig1 controls ErbB activation *in vivo*

a-d) Pharmacological inhibition of ErbB activation restores proliferation in the intestinal epithelium and the crypt size to normal in Lrig1 KO animals. Crypt size and proliferation is visualised by the expression of Ki67. **e-l)** Treatment with Gefitinib rescues the observed effect on the stem cell niche in Lrig1 KO animals. Paneth cells and stem cells are detected by *in situ* hybridisation for *Cryptdin6* and *Olfm4*, respectively. **m-p)** pEgfr levels are reduced upon treatment with the ErbB inhibitor Gefitinib. Detection of activated Egfr (pEgfr) in tissues from Lrig1 WT and KO animals at P10 either untreated (**m** and **n**) and treated with Gefitinib (**o** and **p**). **q-t)** A loss of function Egfr mutant rescues the Lrig1 KO phenotype. Morphologically proliferation has been restored to normal levels in the rescued animals as detected by expression of Ki67 by immunohistochemistry. All Lrig1 KO mice on an $Egfr^{wt/wt}$ background have the expected phenotype (**r**,15 out of 15), however, a large proportion of Lrig1 KO animals heterozygous for the hypomorphic Egfr allele ($Egfr^{wt/wa-2}$) have normal intestinal morphology (**t**, 15 out of 37; p=0.0095) although some still display hyperplasia (**s**). **u)** Model of the role of Lrig1 in stem cell homeostasis as a regulator of ErbB signalling. Scale bars: 50μm (a-t).